Atomistic theory of excitonic fine structure in InAs/InP nanowire quantum dot molecules

M. Świderski and M. Zieliński*

Institute of Physics, Faculty of Physics, Astronomy and Informatics, Nicolaus Copernicus University, Grudziadzka 5, 87-100 Torun, Poland

(Received 10 October 2016; revised manuscript received 16 January 2017; published 6 March 2017)

Nanowire quantum dots have peculiar electronic and optical properties. In this work we use atomistic tight binding to study excitonic spectra of artificial molecules formed by a double nanowire quantum dot. We demonstrate a key role of atomistic symmetry and nanowire substrate orientation rather than cylindrical shape symmetry of a nanowire and a molecule. In particular for [001] nanowire orientation we observe a nonvanishing bright exciton splitting for a quasimolecule formed by two cylindrical quantum dots of different heights. This effect is due to interdot coupling that effectively reduces the overall symmetry, whereas single uncoupled [001] quantum dots have zero fine structure splitting. We found that the same double quantum dot system grown on [111] nanowire reveals no excitonic fine structure for all considered quantum dot distances and individual quantum dot heights. Further we demonstrate a pronounced, by several orders of magnitude, increase of the dark exciton optical activity in a quantum dot molecule as compared to a single quantum dot. For [111] systems we also show spontaneous localization of single particle states in one of nominally identical quantum dots forming a molecule, which is mediated by strain and origins from the lack of the vertical inversion symmetry in [111] nanostructures of overall C_{3v} symmetry. Finally, we study lowering of symmetry due to alloy randomness that triggers nonzero excitonic fine structure and the dark exciton optical activity in realistic nanowire quantum dot molecules of intermixed composition.

DOI: 10.1103/PhysRevB.95.125407

Compared to traditional self-assembled quantum dots [1] nanowire quantum dots [2] reveal several unique spectral features. The high quantum dot shape symmetry [3] combined with the lack of the wetting layer [4] leads to a small or even vanishing excitonic fine structure splitting. The significantly reduced bright exciton fine structure splitting is a key prerequisite for efficient entangled photon pair generation [5,6] with important applications in quantum information and cryptography. High quality, stacking-fault free [7] nanowire quantum dots demonstrate excellent optical properties, with narrow line widths and pure single photon emission [7]. The tailored shape [8] of the nanowire host gives further benefits significantly increasing the light extraction efficiency as compared to quantum dots embedded in bulk.

Single disk shaped InAs/InP nanowire quantum dots have either D_{2d} or C_{3v} [9] symmetry, respectively, for [001] or [111] grown nanowires. Such high symmetry in both cases leads to degenerate bright exciton states and therefore, in principle, to vanishing excitonic fine structure splitting [3,10]. Additionally C_{3v} nanostructures have degenerate ground dark exciton state, whereas in nanostructures of D_{2d} symmetry the dark exciton is split by the exchange interaction. Vanishing bright exciton fine structure in quantum dots may have applications in entangled photon generation [5,6], whereas the control of the dark exciton fine structure and its optical activity may allow for efficient utilization of the dark exciton as a long-lived solid-state qubit [11–13].

Apart from a vast number of single quantum dot studies in the last two decades there has been an extensive experimental effort in the field of double (coupled) quantum dots forming a solid-state analog of a molecular system [10,14–17]. These works included studies of quantum dots in different lateral and vertical configurations [15], including misalignment [18,19] as well as application of external fields [18,20–22]. This experimental effort was assisted by intensive theoretical research [19,23–27].

In this work we focus our attention on the excitonic fine structure of double InAs/InP nanowire quantum dots forming artificial quantum dot molecules [28]. According to our knowledge there has been neither theoretical nor experimental work done in this field. Whereas heterostructures consisting of multiple, thin insertions in a nanowire have already been obtained for other materials (AlGaAs [29] and GaP/GaAs [30]), such double nanowire InAs/InP quantum dots as studied in this work have not been grown yet. There are however no fundamental limits in the vapor-liquid-solid (VLS) growth [31] mechanism of InAs/InP nanowire quantum dots [2,32], and such nanostructures should be achievable in the near future as a natural follow-up of single InAs/InP nanowire quantum dots.

In this paper, using an atomistic tight-binding [33–41] approach, we study single particle and excitonic emission spectra of various double nanowire quantum dot systems as a function of interdot separation and nanowire orientation. We demonstrate pronounced spectral differences between nanowire quantum molecules grown on [001] and [111] substrates. We study cases where double quantum dots either inherit or not the symmetry and spectral prosperities of their single quantum dot constituents. We show significant dark and bright exciton spectra dependence on the interdot distance with a fundamental difference between the weak and the strong coupling regime. We demonstrate nonzero fine structure splitting in [001] quantum dot molecules, as well as a significant increase of the dark exciton optical activity due to the interdot coupling. Finally, for realistic $InAs_xP_{1-x}$/InP nanowire quantum dots we show that effects of alloying [4,42–45] and alloy (lattice) randomness will break the perfect symmetry and contribute to a significant bright exciton splitting.

*mzielin@fizyka.umk.pl

I. COMPUTATIONAL METHODS

Our atomistic calculations consist of several key steps. Since there is 3% lattice mismatch between InAs quantum dots and the InP nanowire, first we calculate strain relaxed positions. We use the atomistic valence force field approach of Keating [46,47] with the minimization of the strain energy performed using the conjugate gradient method [25]. Systems we model are so-called capped or cladded [7] nanowire quantum dots, where the host nanowire diameter (reaching 100 nm in the experiment) is much larger than that of the quantum dots. Therefore we utilize boundary condition for strain calculations assuming InP bulk lattice constant on the nanowire surface. The VFF method is described in more detail in Refs. [48,49] and in our previous papers [25,38–40]. Once the atomic positions are given, we use them to calculate single particle energies with the empirical nearest-neighbor tight-binding model that accounts for strain, spin-orbit interactions, and d orbitals [39,40].

The single-particle tight-binding Hamiltonian for the system of N atoms and m orbitals per atom can be written, in the language of the second quantization, in the following form:

$$\hat{H}_{TB} = \sum_{i=1}^{N}\sum_{\alpha=1}^{m} E_{i\alpha} c_{i\alpha}^{+} c_{i\alpha} + \sum_{i=1}^{N}\sum_{\alpha=1,\beta=1}^{m} \lambda_{i\alpha,\beta} c_{i\alpha}^{+} c_{i\beta} + \sum_{i=1}^{N}\sum_{j=1}^{\text{near.neigh.}}\sum_{\alpha,\beta=1}^{m} t_{i\alpha,j\beta} c_{i\alpha}^{+} c_{j\beta}, \quad (1)$$

where $c_{i\alpha}^{+}$ ($c_{i\alpha}$) is the creation (annihilation) operator of a carrier on the (spin-)orbital α localized on the site i, $E_{i\alpha}$ is the corresponding on-site (diagonal) energy, and $t_{i\alpha,j\beta}$ describes the hopping (off-site, off-diagonal) of the particle between the orbitals on (four) nearest neighboring sites. The summation i goes over all atoms, whereas the summation over j goes over the four nearest neighbors only. α is a composite (spin and orbital) index of the on-site orbital, whereas β is a composite index of the neighboring atom orbital. Coupling to further neighbors is thus neglected, whereas $\lambda_{i\alpha,\beta}$ (on-site, off-diagonal) accounts for the spin-orbit interaction following the description given by Chadi [50] and including only the contributions form atomic p orbitals. Following Ref. [51] we neglect much smaller splittings of excited d orbitals.

We use tight-binding parameters set from Ref. [51] in $sp^3d^5s^\star$ parametrization (explicit parameters are given in Table III on p. 6499 of Ref. [51]). This parametrization utilizes one s, three p, five d, and one excited s^* orbital for each site and each spin component, giving (with spin) total twenty [$m = 20$ in Eq. (1)] spin orbitals per atom. We passivate dangling bonds on the surface to exclude nonphysical (spurious) states. The passivation is modeled by shifting the energy of these bonds high above the conduction band edge so they do not modify states near the band gap [52]. The tight-binding calculation is effectively performed on a smaller domain (subsection of nanowire) than the VFF calculation [52,53]. The number of atoms in the tight-binding simulation is equal to ≈0.5 million, whereas the number of atoms in the VFF simulation reaches over 6 million atoms. These dimensions guarantee convergence of single particle spectra well below one meV [52,53]. More details of the $sp^3d^5s^\star$ tight-binding calculation were discussed thoroughly in our earlier papers [25,38–40].

Due to the small lattice mismatch of InAs and InP, we neglect the piezoelectric effects in the present calculation, following similar arguments by Gong *et al.* [54], who ignore piezoelectricity in the empirical pseudopotential work on InAs/InP quantum dots. Consistently, piezoelectric effects can also be neglected for low aspect ratio [36,55] even in highly-strained quantum dots. We have checked this assumption in nanowire quantum dots by running calculations for several selected cases and by utilizing different models (linear and quadratic) of piezoelectricity. Typically energies of ground excitonic states differ well below 1 meV with respect to cases neglecting piezoelectricity. Moreover, from the symmetry point of view, the piezoelectricity does not affect the overall symmetry of the atomistic tight-binding Hamiltonian, and as such it cannot effectively affect the excitonic fine structure which is the center quantity discussed in this work.

Finally, we follow our single-particle calculation with a many-body calculation to obtain excitonic spectra and in particular excitonic fine structure. The Hamiltonian for the interacting electrons and holes can be written in second quantization as [56]:

$$\hat{H}_{ex} = \sum_i E_i^e c_i^\dagger c_i + \sum_i E_i^h h_i^\dagger h_i + \frac{1}{2}\sum_{ijkl} V_{ijkl}^{ee} c_i^\dagger c_j^\dagger c_k c_l + \frac{1}{2}\sum_{ijkl} V_{ijkl}^{hh} h_i^\dagger h_j^\dagger h_k h_l - \sum_{ijkl} V_{ijkl}^{eh,\text{dir}} c_i^\dagger h_j^\dagger h_k c_l + \sum_{ijkl} V_{ijkl}^{eh,\text{exchg}} c_i^\dagger h_j^\dagger c_k h_l, \quad (2)$$

where E_i^e and E_i^h are the single particle electron and hole energies, obtained at the single particle stage of calculations, and V_{ijkl} are Coulomb matrix elements [38,41]. For the single exciton (electron-hole pair) the above equation is reduced to:

$$\hat{H}_{ex} = \sum_i E_i^e c_i^\dagger c_i + \sum_i E_i^h h_i^\dagger h_i - \sum_{ijkl} V_{ijkl}^{eh,\text{dir}} c_i^\dagger h_j^\dagger h_k c_l + \sum_{ijkl} V_{ijkl}^{eh,\text{exchg}} c_i^\dagger h_j^\dagger c_k h_l, \quad (3)$$

with no electron-electron and hole-hole interactions since we deal with a single electron and hole. The many-body Hamiltonian for the exciton is solved using the configuration interaction (CI) approach [38,57].

Coulomb matrix elements (Coulomb direct and exchange integrals) are calculated according to procedure given in Ref. [38]. This method starts with the tight-binding wave function is given in the form of linear combination of atomic orbitals (LCAO):

$$\phi_i = \sum_{\vec{R},\alpha} b_{\vec{R}\alpha}^i |\vec{R}\alpha\rangle, \quad (4)$$

where $\vec{R}\alpha$ is the α (spin-)orbital localized on atom $\vec{R}$, and $b_{\vec{R}\alpha}^i$ is the LCAO expansion coefficient. Then by utilizing a series of approximations [37,38] (such as the two-center approximation) one gets an approximate form of Coulomb

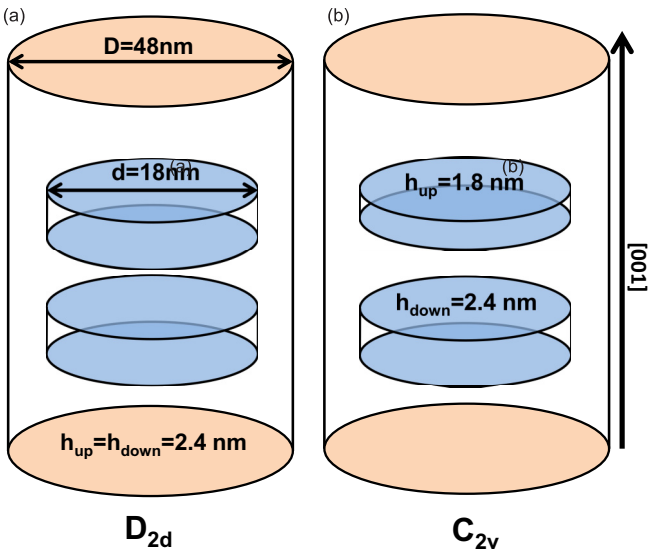

FIG. 1. Schematics of a nanowire quantum dot molecule formed by two identical (a) and two nonidentical (b) disk shaped InAs quantum dots embedded in a [001] oriented InP substrate.

matrix elements [38]:

$$V_{ijkl} = \sum_{\vec{R}_1} \sum_{\vec{R}_2 \neq \vec{R}_1} \left[\sum_{\alpha_1} b^{i*}_{\vec{R}_1\alpha_1} b^{l}_{\vec{R}_1\alpha_1} \right] \left[\sum_{\alpha_2} b^{j*}_{\vec{R}_2\alpha_2} b^{k}_{\vec{R}_2\alpha_2} \right] \times \frac{e^2}{\epsilon |\vec{R}_1 - \vec{R}_2|} + \sum_{\vec{R}_1} \sum_{\alpha_1\alpha_2\alpha_3\alpha_4} b^{i*}_{\vec{R}_1\alpha_1} b^{j*}_{\vec{R}_1\alpha_2} b^{k}_{\vec{R}_1\alpha_3} b^{l}_{\vec{R}_1\alpha_4} \times \langle \vec{R}_1\alpha_1, \vec{R}_1\alpha_2 | \frac{e^2}{|\vec{r}_1 - \vec{r}_2|} | \vec{R}_1\alpha_3, \vec{R}_1\alpha_4 \rangle, \quad (5)$$

where α is the orbital index and $\vec{R}_i$ denotes the position of the ith atom.

The first term is the long-range, bulk-screened (ϵ), a contribution to the two-center integral built from the monopole-monopole interaction [58,59] of two charge densities localized at different atomic sites. The second term is the on-site unscreened part, calculated by direct integration using atomic (Slater) orbitals [33,34]. This approach is justified by the fact that the screening (Thomas-Fermi) radius (≈2–4 Å) is on the order of bond length [34,60] resulting in the nearly bulk screening of off-site (long-range) terms and limited screening of on-site (short-range) contribution. Since in this work we aim at modeling of quantum dots well embedded inside nanowires and separated from the surface by a thick cladding, we neglect effects due to image charges buildup on a nanowire surface.

II. [001] ORIENTED NANOWIRE

Let us start with a quantum dot molecule formed by two identical InAs disk-shaped quantum dots of 2.4 nm (8 monolayers) height and 18 nm diameter, grown on a [001] oriented InP nanowire (Fig. 1). The nanowire diameter is 48 nm. In the vertical (growth) dimension we account for a section of a nanowire which is 96 nm long. Such length is sufficient for the converged single particle and excitonic

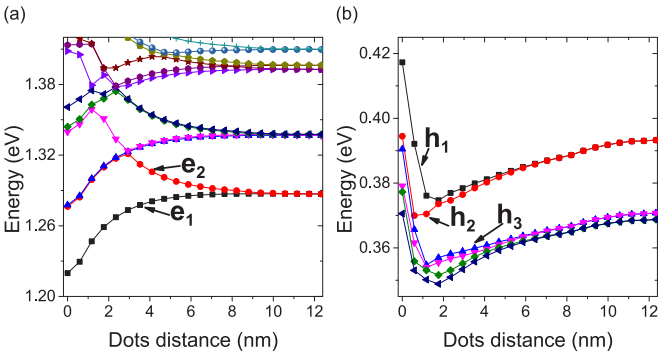

FIG. 2. Single particle electron (a) and hole (b) spectra calculated for a nanowire quantum dot molecule formed by two identical (see the text) disk shaped InAs quantum dots on a [001] oriented InP substrate.

spectra [53]. Figure 2 shows the evolution of a single particle electron and hole spectra for this system as a function of the interdot separation. The corresponding charge densities (for two interdot separations) are shown in Fig. 3 for electrons and

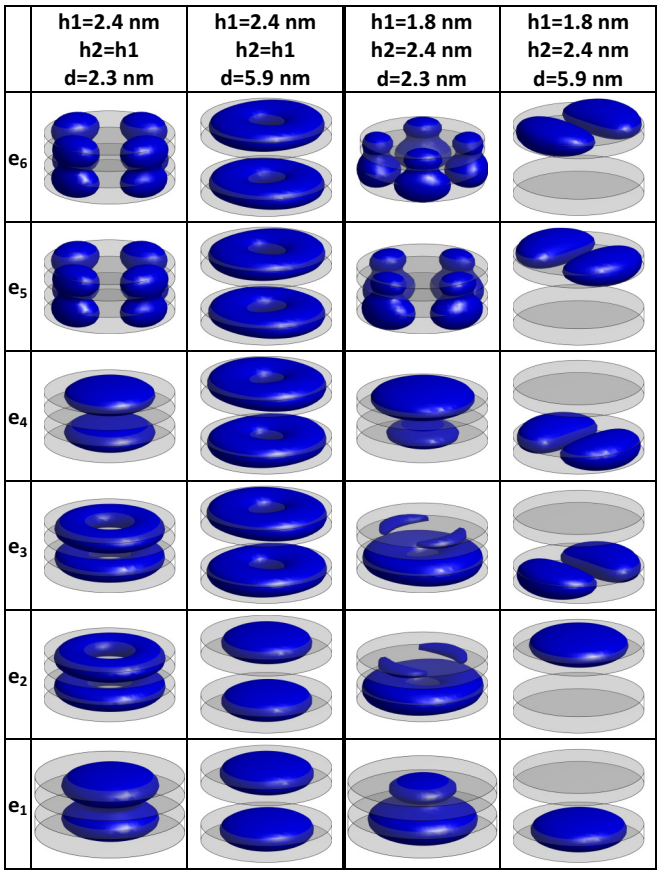

FIG. 3. Single-particle electron probability density isosurfaces for InAs/InP nanowire quantum dots molecule formed by two disk shaped InAs quantum dots of the same (left columns) and different heights (right columns) grown on a [001] oriented InP substrate. Densities are calculated at different (2.3 and 5.9 nm) interdot distances. Isosurfaces enclose 70% of the probability densities. Ground electron states (e_1) are shown in the bottom row.

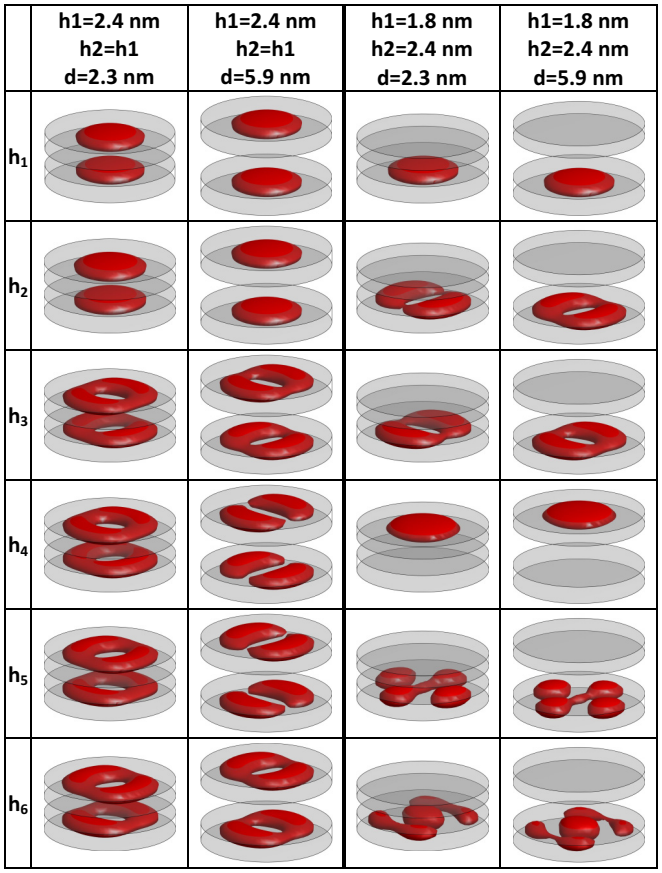

FIG. 4. Single-particle hole probability density isosurfaces for InAs/InP nanowire quantum dots molecule formed by two disk shaped InAs quantum dots of the same (left columns) and different heights (right columns) grown on [001] oriented InP substrate. Densities are calculated at different (2.3 and 5.9 nm) interdot distances. Isosurfaces enclose 70% of the probability densities. Ground hole states (h_1) are shown in the top row.

in Fig. 4 for holes. We note that Figs. 3 and 4 contain additional charge densities for a case of nonidentical quantum dots that will be discussed later in the text. These densities are shown here for comparison and will be discussed in detail in the next section.

In a wide range of the interdot distances the ground (e_1) and the first-excited (e_2) electron states are molecular-like [25,61] orbitals of bondinglike and antibonding character, correspondingly. These two lowest electron states are formed from the s-like single quantum dot electron ground states, whereas similar pairs of molecularlike orbitals are also present for excited states of p and d character (Fig. 3). The simple picture gets more complicated for smaller interdot separations, e.g., at 3 nm there is a level crossing of antibonding s state with two excited p-like states. With even further reduced interdot spacing (≈1 nm) the single particle electron spectra converges to the characteristic shell structure of a single quantum dot [1].

Contrary to electron states, the hole behavior [Fig. 2(b)] is far from trivial. Firstly, for interdot distances larger than several nanometers holes show only weak electronic coupling and therefore there is only a small splitting between the two lowest holes states. This effect could be understood in terms of

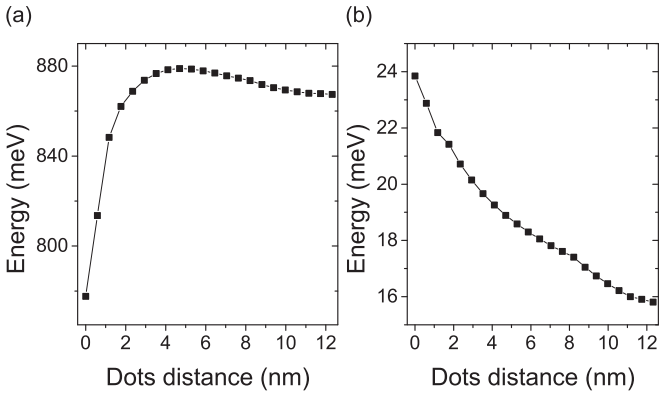

FIG. 5. Evolution of (a) ground exciton state energy and (b) an electron-hole Coulomb direct integral calculated for electron and hole occupying their ground states for a nanowire quantum dot molecule formed by two identical (see the text) disk shaped InAs quantum dots on a [001] oriented InP substrate.

larger effective mass of a hole, therefore significant hole state localization in the quantum dot area and thus reduced wave function leakage into the barrier. In particular, the ground-first excited hole states splitting reaches only 2 meV for ≈2.3 nm interdot distance, with an apparent level crossing at ≈1.8 nm, where the splitting is 1.1 meV. Interestingly, despite reduced splittings, the long-range coupling between quantum dots leads to an overall downshift of hole state energies, reaching nearly 20 meV when comparing the ground state energy at 12 and 2 nm separations. That redshift was not present when we ran auxiliary calculation (not shown here for brevity) with strain artificially neglected [25]. Therefore we conclude that strain is directly responsible for this effect. With smaller interdot distances the hole level structure reverses the trend and converges to that of a single ("merged") quantum dot of twice the height (i.e., 4.8 nm).

We note that such hole states spectra (in particular in the medium and strong coupling regime) obtained by a multiband calculation is qualitatively and quantitatively different from a single band model [61], where the structure of hole levels could be approximated by a simplified 2×2 Hamiltonian model, similarly to the electron states. Such a simple approximation has limited applications for a realistic description of hole levels in quantum dot molecules, and it has to be augmented with additional information originating from a more refined multiband calculation that accounts for strain and spin-orbital interaction [20,62]. Secondly, the ground molecular hole is of antibonding character [20,25,26,62] in a large range of interdot distances. The analogous effect of the antibonding ground hole state has been theoretically [25,26] predicated for self-assembled quantum dot molecules and confirmed by subsequent experimental studies [18,20].

In a typical photoluminescence experiment one does not observe single particle spectra but rather the recombination of an interacting electron-hole pair, the exciton. Figure 5(a) shows the evolution of the ground exciton state energy as a function of the interdot separation. With the distance reduction from 10 to 4 nm the excitonic ground state energy is somewhat increased due to opposing evolution of the ground electron and hole states, and the holes trend dominating the single particle

energies evolution. Below 4 nm interdot separation there is a pronounced reduction of the excitonic energy being a hallmark of the interdot coupling, affecting both electrons and holes and interactions between them. In particular, the reduction of the interdot separation leads to the increased electron-hole attraction between particles occupying quasimolecular states as shown in Fig. 5(b). The shorter the distance between quantum dots forming a molecule, the stronger the spatial contraction of the single particle wave functions and the electron-hole overlap, leading in the end to the increase of a Coulomb attraction between these charge carriers. This, apart from the dominant single particle contribution, will further reduce the excitonic energy for smaller quantum dot distances since the Coulomb attraction enters the excitonic Hamiltonian with a negative sign [1].

The antibonding character of the ground hole state in a nanowire quantum dot molecule manifest itself by a nearly vanishing (i.e., our calculations indicate it is reduced by $\approx 10^{-4}$ factor as compared to the single quantum dot) optical dipole matrix element for the in-plane polarized transitions between the ground electron and the ground hole state. On the other hand, the optical matrix element is nonzero for the in-plane polarized transitions between the first excited ("bonding") hole state and the ("bonding") ground electron state. In other words, in a wide range of quantum dot distances, considering the in-plane polarizations and single particle transitions, the ground hole state is optically nonactive, whereas the excited hole state has strong optical activity.

Things get even more complicated when accounting for the electron-hole exchange interaction. Typical self-assembled or single nanowire quantum dots have a very characteristic excitonic fine structure [3,10] formed by a low energy doublet of excitonic states showing practically zero optical activity, hence known as the dark exciton states, and a pair of two optically active states known therefore as the bright exciton states. Theses four excitonic states are dominated by configurations involving electron and hole ground state with different ("up", "down") spin orientations of electron and hole. The optical selection rules stem from the spin properties of electron and hole states [10] combined with group-theoretical arguments [3,63,64].

A new, characteristic, and peculiar feature of nanowire quantum dot molecules is in fact related to their excitonic fine structure spectra as will be shown in the following part of the paper. Double quantum dots should in principle inherit symmetry properties of their single dot constituents. In particular, a quantum dot molecule formed by two identical [001] grown nanowire quantum dots should be described by the same point group (D_{2d}) as the individual components. In such a case, as confirmed by our atomistic calculations, the "bright" exciton fine structure splitting (splitting between the second and the third excited excitonic state) is zero for all considered distances as demanded by the symmetry [3]. The "dark" exciton (the ground and the first excited states) splitting is nonzero, however it is small, typically well below 1 μeV.

As mentioned above, in a nanowire quantum dot molecule formed by identical quantum dots in a wide range of interdot distances the ground hole state is of antibonding character. As a result the lowest two excitonic states have weak optical activity due to spin selection rules, whereas the two nominally "bright"

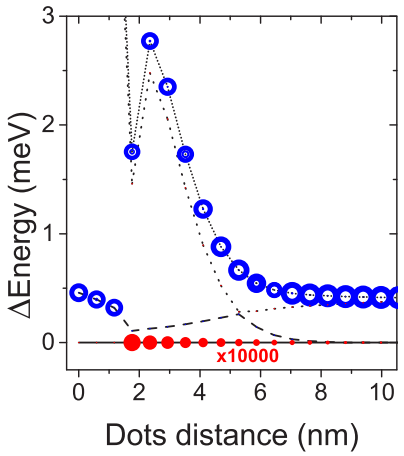

FIG. 6. Energies and oscillator strengths of several lowest exciton states shown with respect to the ground exciton states (solid line). The ground and the first excited ("dark") exciton states are quasidegenerate and are denoted by a solid line, whereas the second and the third excited exciton states are degenerate and are denoted by a dashed line. Analogously, the dotted line corresponds to the fourth and fifth excited exciton states, whereas the dashed-dotted line corresponds to the sixth and seventh excited excitonic states. The blue/empty circles represent the transitions polarized in the growth plane, whereas the red/full circles represent transitions polarized along the growth direction. The size (area) of the circles is proportional to the oscillator strength. Energies are measured with respect to the ground excitonic ("dark") state.

states, i.e., the second and the third excited excitonic states, are in fact practically dark (in a broad range of interdot separations) because of the vanishing overlap of the antibonding ground hole state and the bonding ground electron state (Fig. 6). In effect, the quadruplet of four lowest excitonic states reveals only a very weak optical activity for the in-plane polarized transition, as compared to a single quantum dot case. However, the optical properties of higher excited excitonic states (fourth to seventh excited) resembles that of a traditional quantum dot, with two dark states (fourth and fifth excited) and two optically active, bright states (six and seventh excited). At 1.8 nm separation there is an apparent state crossing and for smaller distances and strongly coupled quantum dots the ground hole state and thus the excitonic spectra resemble that of a typical for single D_{2d} quantum dot, with two dark (quasidegenerate) and two bright (exactly degenerate) excitonic states (Fig. 6).

Interestingly, apart from the reduction of the optical activity of low-lying bright states, the quasimolecular character of the ground hole state has a pronounced effect on the dark exciton. We found that one of the dark exciton states gets nonzero oscillator strength corresponding to z (out-of-plane) polarized light (red/full circles in Fig. 6). This weak yet non-negligible emission grows with the reduction of the interdot separation reaching its maximum at 1.8 nm (Fig. 7).

In order to analyze this effect let us first move back to the case of a single quantum dot. In such a system, in a reasonable approximation, the ground electron and hole state have s-type envelopes, both in the vertical (growth) and in lateral directions. Moreover the electron wave function is dominated by s-type atomic orbitals, whereas the (heavy) hole wave

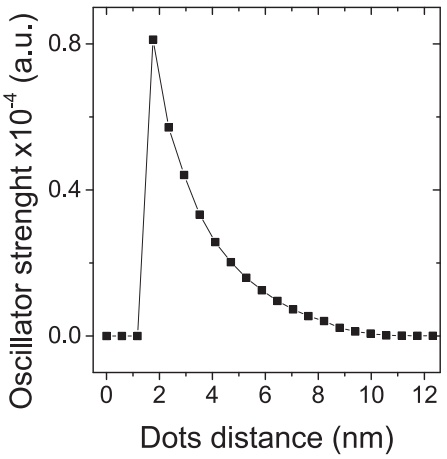

FIG. 7. The evolution of the total oscillator strengths corresponding to the two lowest ("dark") excitonic states as a function of interdot separation. The oscillator strength unit is normalized to the strongest bright exciton of a single (merged, $h = 4.8$ nm) quantum dot ($d = 0$).

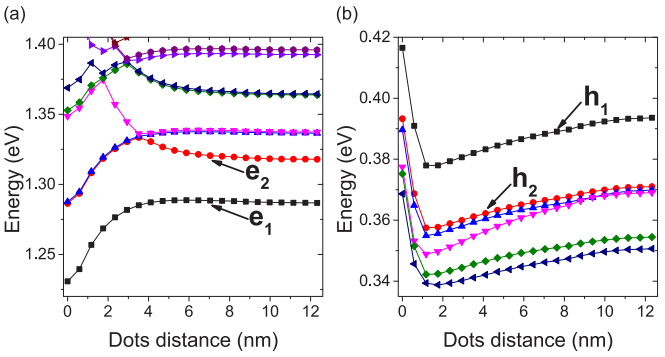

FIG. 8. Single particle electron (a) and hole (b) spectra calculated for a nanowire quantum dot molecule formed by two disk shaped InAs quantum dots of different height (see the text) on [001] oriented InP substrate.

function consists predominately of p_x and p_y atomic orbitals. Therefore, in the framework of such an approximation, the out-of-plane (z) polarized transition is forbidden by selection rules.

Going beyond this approximation and accounting for the actual atomistic symmetry the dark exciton transitions become optically allowed, e.g., for C_{2v} or C_{3v} quantum dots even for an exciton with a pure heavy-hole character [63]. However in single quantum dots of cylindrical symmetry these transitions remain very weak, whereas they are exactly zero for D_{2d} single quantum dots [3].

From a theoretical point of view one way of increasing optical activity of the dark exciton is the deformation of quantum dot shape from the cylindrical base to the elongated one [4,65] or even more peculiar shape distortion [13]. In the former case one achieves the increased dark excitonic activity by breaking the rotational symmetry and increasing the content of the light-hole contribution [66]. In the quantum dot molecule the ground hole state remains however of heavy-hole character, with a small (few percent) light-hole contribution that does not change significantly in a wide range of interdot spacings [20] as confirmed by our calculations. Therefore the increase of the dark exciton activity cannot be contributed to the increase of the light-hole admixture in the hole ground state.

We reiterate that the [001] oriented quantum dot molecule has D_{2d} symmetry. For a single quantum dot system of such symmetry (with the s-like heavy-hole dominated ground hole state) one expects by both effective mass and group theoretical arguments [3] two dark excitonic states to show no optical activity. However in the case of a molecule we deal with an antibonding (antisymmetric) ground hole state. Therefore the single particle ground hole state is no longer a quasi-s-like wave function as in the case of a single quantum dot, but its character is altered by the presence of the second quantum dot leading to a formation of quasimolecular orbital. In effect the nominally "dark" transition gains significant oscillator strength, at the maximum reaching a non-negligible 10^{-4} fraction of the bright exciton (Fig. 7).

The dark exciton forms therefore a long-lived, yet optically addressable state with potential applications in quantum information and optics [11–13]. Recently several new schemes for tailoring dark exciton optical activity in single quantum dots have been presented [13,65]. Here we present a different growth-controlled mechanism, namely the utilization of coupling between quantum dots in a vertically stacked molecule. We also note that our results related to the dark exciton spectra should be to some extent generalizable to other [001] quantum dot molecules revealing antibonding ground states, such as self-assembled InAs/GaAs vertically stacked quantum dots [18,20].

Results obtained in this section were obtained for an idealized system of two identical quantum dots forming a molecule. Contrary to atomic physics, practically no two quantum dots are ever the same and individual dots will (to some extent) always vary in size and composition. It is thus of high importance to verify how this will affect their excitonic properties.

Nonidentical quantum dots

In what follows we study a case of two quantum dots of different height (2.4 nm and 1.8 nm; 8 and 6 InAs monolayers correspondingly) but of the same diameter (right-hand side of Fig. 1). The assumption of nearly identical diameters of both quantum dots in a molecule is reasonably justified by the VLS growth mechanism [31,32,67], where the quantum dot diameter is fixed by the dimension of the host InP nanowire, whereas the height of the quantum dot can be quite effectively controlled. In the last part of our paper, we will move our attention to a yet more realistic system of intermixed composition.

Figure 8 shows electron and hole single particle spectra of two nonidentical quantum dots molecules. At large interdot separation electron states remain effectively uncoupled, with the energy spacing of 31 meV's between e_1 and e_2 due to difference in confinement (height) of individual quantum dots. The ground electron state (e_1) is localized within the larger quantum dot, whereas the first excited state (e_2) is localized in the smaller quantum dot (right two columns of Fig. 3). At distances below 6 nm quantum dots couple strongly and

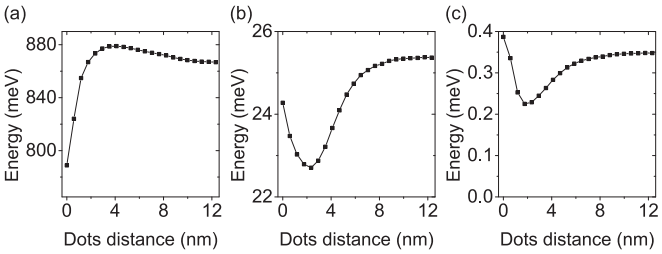

FIG. 9. Evolution of (a) ground excitonic state energy and (b) electron-hole Coulomb direct and (c) electron-hole exchange integrals calculated for electron and hole occupying their ground states for nanowire quantum dot molecule formed by two nonidentical (see the text) disk shaped InAs quantum dots on a [001] oriented InP substrate.

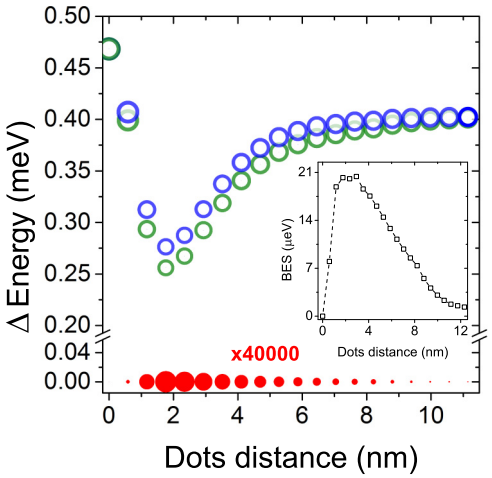

FIG. 10. The bright and dark exciton energy and the optical spectra calculated for a nanowire quantum dot molecule formed by two disk shaped InAs quantum dots of different height (see the text) on [001] oriented InP substrate. Blue and green circle correspond to [110] and [1$\underline{1}$0] orthogonal polarizations. Red circles correspond to [001] (z) polarized light. The size (area) of the circles is proportional to the oscillator strength. Energies are measured with respect to the ground excitonic ("dark") state. The inset shows the bright exciton splitting as a function of quantum dots distance.

electron states form a molecularlike orbital. On the other hand, the hole states do not couple in a straightforward manner and do not create a simple molecular orbital (right two columns of Fig. 4). The ground state of a hole (h_1) originates from a larger ($h = 2.4$ nm) single quantum dot ground state and remains localized in the larger dot in most interdot separations. Similarly, the first excited hole state of the molecule originates from a smaller ($h = 1.8$ nm) single quantum dot ground state and is separated by ≈20 meV from the ground state of a molecule. Its energy falls closely to two excited hole states of the larger quantum dot forming thus a group of three closely spaced excited states [Fig. 8(b)].

Figure 9(a) shows the evolution of the ground excitonic state energy as a function of the interdot separation. This dependence strongly resembles that for a case of identical quantum dots molecule, with a pronounced energy reduction due to interdot coupling at distances smaller than 4 nm. A more peculiar and a different behavior can however be observed for electron-hole Coulomb direct [Fig. 9(b)] and ("isotropic") exchange interaction [Fig. 9(c)]. The reduction of interdot distance leads to the delocalization of the electron state and the leakage of the electron probability density into the smaller quantum dot (Fig. 4), whereas the hole charge density remains effectively localized in the larger dot and uncoupled from the smaller dot. This effectively reduces the electron-hole spatial overlap and thus Coulomb direct and exchange interaction. The latter term is responsible for the splitting of the bright and dark excitonic doublets and hence is sometimes denoted as the "isotropic" electron-hole exchange, contrary to the "anisotropic" exchange responsible for the bright exciton doublet splitting. We point out however that these terms (isotropic, anisotropic) have in fact mostly historical meaning, since modern understanding of the fine structure splitting focuses on the role of the overall symmetry rather than shape elongation ("anisotropy") of quantum dots only.

It should be also noticed that despite cylindrical shapes and identical quantum dot diameters, the system of different height [001] grown quantum dots lacks vertical roto-inversion symmetry [3] and the overall quantum molecule symmetry is reduced to C_{2v} (Fig. 1). Such low symmetry leads to a nonzero fine structure splitting of both dark and bright excitons [3]. Figure 10 shows the details of the excitonic fine structure and the optical spectra of bright and dark excitons calculated for the discussed system. The bright exciton splitting is different from zero and is equal to 1.3 μeV for the largest shown interdot distance. Importantly, the bright exciton splitting increases quasimonotonically with the reduction interdot coupling reaching its maximum of ≈20 μeV for the 3 nm interdot spacing (inset of Fig. 10). The further reduction of quantum dots spacing reverses the trend, and the bright exciton splitting is again exactly zero for the case of zero interdot distance, i.e., effectively for the merged (single) quantum dot of height equal to 4.8 nm and therefore of D_{2d} symmetry. This peculiar effect of distance dependent bright exciton splitting is a direct effect of the formation of asymmetric molecularlike orbital of the electron ground state. For the asymptotic case of the large interdot separation the electron ground state is localized entirely within its parental (large) quantum dot and is of approximately s-like symmetry that practically keeps the roto-inversion symmetry operations (D_{2d} symmetry). With the reduction of the interdot distance, the overall symmetry is effectively reduced to C_{2v} and the ground electron state acquires a tail in the second (smaller) dot region due to the interdot coupling (Fig. 3). The molecular state becomes strongly asymmetrical for the small interdot separation. This vertical asymmetry, i.e., different state localization in both quantum dots, is then directly responsible for the bright exciton splitting as shown in Fig. 10.

To summarize, the leakage of the electron charge density out of the larger quantum dot and into the smaller dot has a peculiar effect on the electron-hole exchange interaction. It leads to reduced ("isotropic") electron-hole exchange interaction, that is seen in Fig. 10 as a dip in the bright exciton energy measured from the dark exciton ground state, and it induces bright exciton splitting ("anisotropic" electron-hole exchange) seen as the splitting between excitonic lines corresponding to different polarizations (shown as well in Fig. 10). In both cases

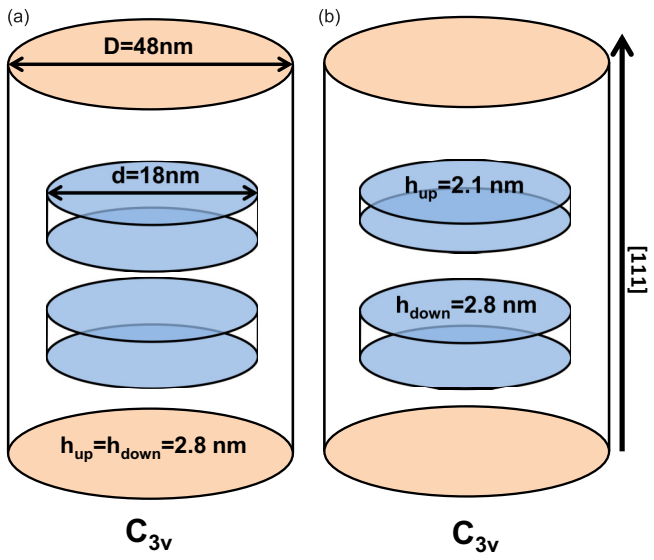

FIG. 11. Schematics of nanowire quantum dot molecule formed by two identical (a) and two nonidentical (b) disk shaped InAs quantum dots embedded in a [111] oriented InP substrate.

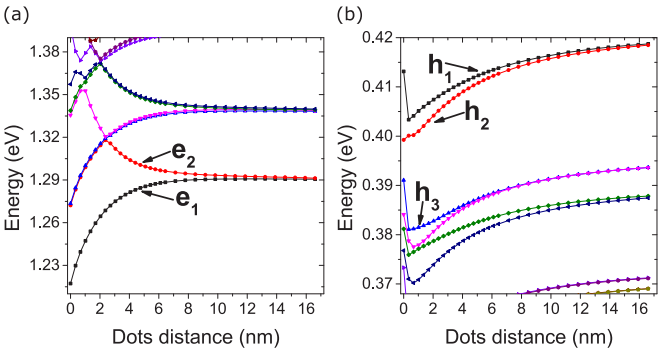

FIG. 12. Single particle electron (a) and hole (b) spectra calculated for a nanowire quantum dot molecule formed by two identical (see the text) disk shaped InAs quantum dots on [111] oriented InP substrate.

this phenomenon reaches maximum for ≈1.8 nm interdot spacing and then the trend is reversed as the quantum dots merge and the entire system regains its symmetry D_{2d}.

Importantly, for a case of nonidentical quantum dots, we again observe the pronounced effect of reduced interdot separation on the dark exciton spectra (red/full circles in Fig. 10). As mentioned above the hole states coupling appears minimal, however the formation of quasimolecular orbitals is apparently effective enough to commence significant dark exciton brightening as shown in Fig. 10. We note however the molecule of two nonidentical [001] quantum dots has C_{2v} symmetry. For such a case the optical activity of the dark exciton is allowed [63] already for single quantum dots, whereas in the case of identical quantum dots and D_{2d} symmetry the optical activity of the dark exciton was possible due to formation of the quasimolecular (antibonding) ground hole state. Despite different molecule symmetry (C_{2v} versus D_{2d}) the effect is similar to that of identical dots, with the dark exciton emission polarized in the growth direction, however it is weaker by approximately factor four, most likely due to reduced coupling between quantum dots of different heights.

Finally, we emphasize that the realistic calculation of the excitonic fine structure, accounting both for energy splittings and polarizations, cannot be in straightforward manner achieved by simple (1-band) effective mass theory. These effects come from low overall nanosystem symmetry, including both shape and lattice and can only be captured by a refined method, such as an atomistic approach such as used in this work, or multiband [28,63,68–71] $k * p$ treatment to account for the correct atomistic symmetry.

III. [111] ORIENTED NANOWIRE—C_{3v} QUANTUM MOLECULES

Previous section focus was on studies of nanowire quantum molecules grown on a [001] substrate, whereas nanowire quantum dots are typically grown either on a [111] zinc-blende oriented nanowire, or [1111] wurtzite nanowires [7]. Atomistic modeling of wurtzite InAs/InP nanostructures presents a significant practical challenge, predominantly due to lack of reliable data (fitting targets) for bulk InAs and InP in wurtzite phases [72,73]. For example, the reported values of InP wurtzite bulk band gaps vary from 1.4 to 1.6 eV. Fortunately, both [111] zinc-blend and [1111] wurtzite nanowires share the same symmetry group, i.e., C_{3v} (Fig. 11). Therefore, whereas one should expect a quantitative difference between systems grown in both crystal phases (such as different effective band gaps), the qualitative results (that depend heavily on the symmetry) should be comparable.

Figure 12 shows electron and hole single particle spectra calculated for a [111] oriented nanowire quantum dot molecule consisting of an identical quantum dot of $h = 2.8$ nm (8 monolayers along the [111] direction) and $d = 18$ nm. At first glance, for the [111] case the single particle spectra are very similar to [001] with distance dependent and pronounced level coupling, and the formation of molecular orbitals for electron states, and limited coupling of hole states. However a further inspection (Figs. 13 and 14) of the corresponding single particle charge densities reveals a fundamental difference between both orientations. In particular, for the [111] case eigenstates of a tight-binding Hamiltonian transform according to irreducible representations of the C_{3v} group, which does not contain the rotoinversion ('improper rotation') operation [3]. The lack of inversion symmetry and the resulting vertical asymmetry can in fact be considered a hallmark of [111] grown nanosystems of C_{3v} symmetry.

As a result, we observe that even for the case of quantum molecule build from two identical quantum dots, the system has vertical asymmetry and the single particle ground electron state prefers to localize in the bottom (with respect to the [111] direction) quantum dot, whereas the single particle ground hole state tends to localize in the upper quantum dot.

By running calculations with strain effects accounted for and strain effects artificially neglected, we found that this curious effect quantitatively stems from strain. It should be emphasized that whether strain is included or neglected the point group symmetry of a molecule remains the same (C_{3v}). Despite being relatively small (as compared to InAs/GaAs

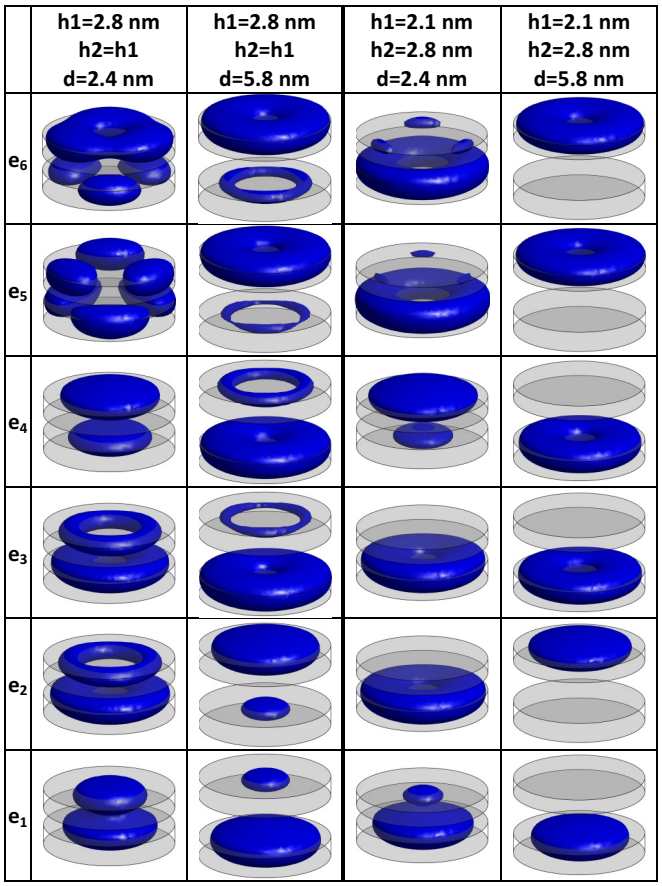

FIG. 13. Single-particle electron probability density isosurfaces for an InAs/InP nanowire quantum dots molecule formed by two disk shaped InAs quantum dots of the same (left columns) and different heights (right columns) grown on a [111] oriented InP substrate. Densities are calculated at different (2.3 and 5.9 nm) interdot distances. Isosurfaces enclose 70% of the probability densities. Ground electron states (e_1) are shown in the bottom row.

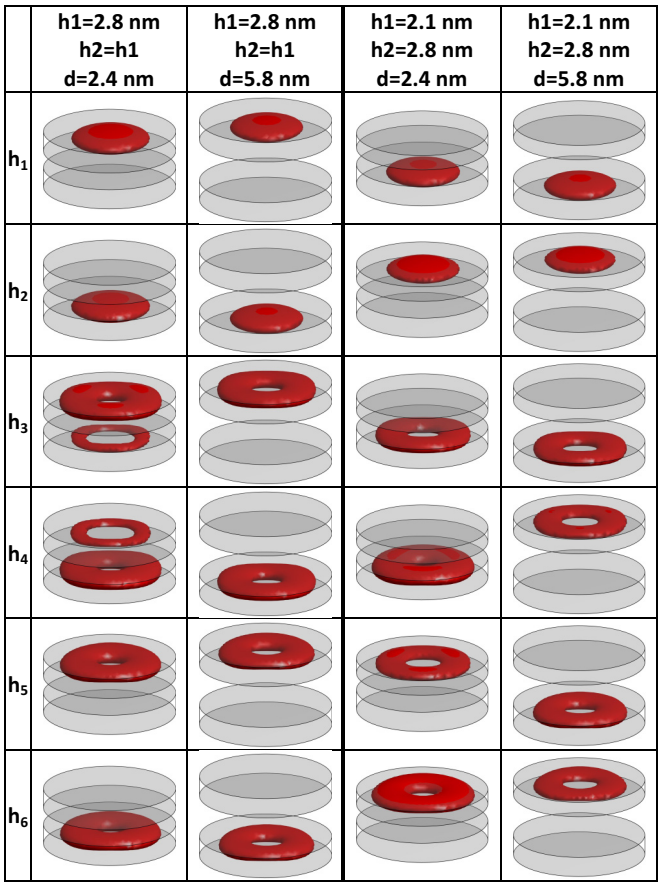

FIG. 14. Single-particle hole probability density isosurfaces for an InAs/InP nanowire quantum dots molecule formed by two disk shaped InAs quantum dots of the same (left columns) and different heights (right columns) grown on a [111] oriented InP substrate. Densities are calculated at different (2.3 and 5.9 nm) interdot distances. Isosurfaces enclose 70% of the probability densities. Ground hole states (h_1) are shown in the top row.

systems) the 3% lattice mismatch between InAs quantum dots and InP nanowire has an important effect [40] on spectra of InAs/InP nanostructures. In our case of identical [111] double quantum dots with strain effects artificially neglected we regain (not shown here) almost symmetrical molecularlike orbitals of the ground electron and holes states, whereas with strain effects accounted for the charge density resembles the molecular orbital of the heteroatomic system as seen in Figs. 13 and 14. Strain thus effectively enhances vertical asymmetry reducing formation of a quasimolecular orbital for electron and hole states in [111] quantum dot molecules.

An analogous effect of increased single particle state localization in one of the coupled quantum dots was theoretically reported [74] in InAs/GaAs quantum dot molecules. Yet, that effect was observed for hole states only and most importantly for quantum dots of C_{2v} symmetry (e.g., [001] lens shaped quantum dot on a wetting layer), i.e. that is with the inversion symmetry reduced by the shape of a nanostructure. Here we report the increased spatial localization in one of the quantum dots for high quantum dot shape symmetry (disk) whereas the symmetry is effectively reduced to C_{3v} by the presence of the lattice. Again, we emphasize that both single and double [111] quantum dots have the same overall C_{3v} symmetry.

Since the ground electron and hole states are spatially separated this should have an important effect on the final excitonic spectra, in particular on the oscillator strengths due to reduction of electron-hole overlap. However, that ground excitonic state is not built from excitonic configuration involving electron and hole ground state, i.e., $|e_1h_1\rangle$ (these are actually four configurations with different electron and hole spin projections), but rather the ground excitonic state is dominated by a configuration involving the ground electron state and the hole in the first excited state, i.e., $|e_1h_2\rangle$. The $|e_1h_2\rangle$ configuration is effectively built from both the electron and the hole state localized in the lower quantum dot. The $|e_1h_1\rangle$ configuration has lower single particle (kinetic) energy than $|e_1h_2\rangle$ since by definition h_2 is an excited state [75]. However when accounting for the Coulomb interaction, the electron-hole attraction between states localized in different quantum dots, i.e., e_1 and h_1 is weaker than that between the electron and the hole in the same quantum dot, i.e., e_1 and h_2. This is illustrated in Fig. 15 which shows that Coulomb attraction J_{e1h2} between e_1 and h_2 states typically

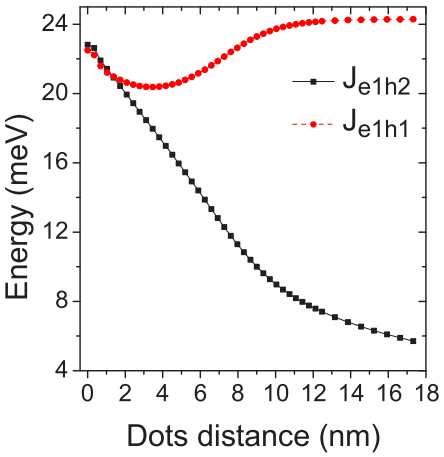

FIG. 15. Electron-hole Coulomb direct integral calculated for electron and hole occupying their ground states (J_{e1h1}), and electron in the ground state, whereas the hole is in the first excited state (J_{e1h2}). Note that Coulomb attraction enters the excitonic Hamiltonian with a negative sign.

ranges between 20 and 24 meV. On the other hand Coulomb attraction J_{e1h1} between ground electron e_1 and hole h_1 states is as small as ≈6 meV for highly separated quantum dots, and it exceeds J_{e1h2} only for strongly coupled quantum dots, separated by less than 2 nm. Since the Coulomb interaction between electron and hole is attractive, it effectively enters the excitonic Hamiltonian with a negative sign and thus reduces $|e_1h_2\rangle$ configuration ("Hartree") energy with respect to $|e_1h_1\rangle$ (Fig. 16). Therefore after accounting for interactions the lowest energy configuration is $|e_1h_2\rangle$ and it is optically active.

Contrary to [001] systems, the lack of the rotoinversion symmetry is not responsible for the vanishing excitonic fine structure splitting since quantum dot molecules maintain the same C_{3v} symmetry as the single nanowire quantum dots (Fig. 11). Therefore, the vertical asymmetry of single particle

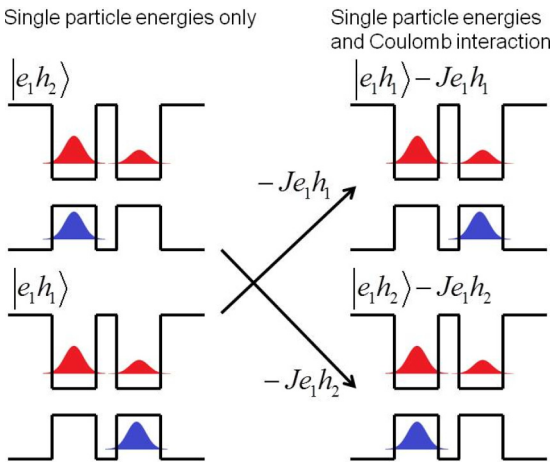

FIG. 16. Schematics illustrating reordering of energies of electron-hole configurations by the Coulomb interaction. e_1 corresponds to the ground electron states, and h_1 and h_2 correspond to the ground hole and the first excited state, respectively. J is the Coulomb integral.

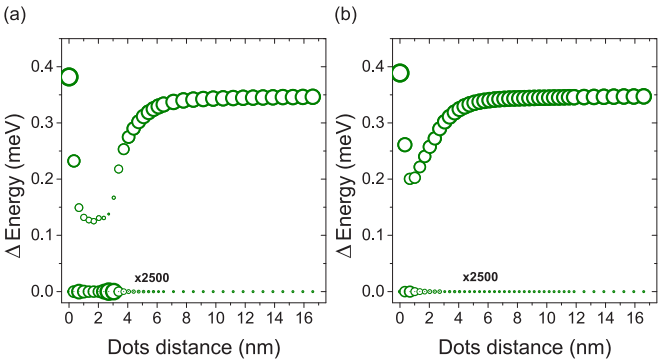

FIG. 17. The bright and dark exciton energy and optical spectra calculated for nanowire quantum dot molecule formed by (a) two identical disk shaped InAs quantum dots (see the text) on [111] oriented InP substrate and (b) two disk shaped InAs quantum dots of different height. The size (area) of the circles is proportional to the oscillator strength. Energies are measured with respect to the ground excitonic ("dark") state.

orbitals cannot trigger the bright (or dark) exciton splitting in [111] quantum dot molecules. Figure 17(a) shows the details of the excitonic fine structure and the optical spectra of this system. Interestingly we observe a dip in the exchange splitting between bright and dark doublet similar to a case [001] nonidentical quantum dot molecule. Here, the [111] are identical, however lacking inversion symmetry. Thus the reduction of distance between dots leads to an increase of coupling and formation of the delocalized electron state, while keeping the hole states localized in the upper dot. As discussed earlier this reduces the bright-dark exciton exchange splitting. Importantly however, both dark and bright excitons remain degenerate at all considered distances.

Finally, we note the dark exciton [111] quantum dot molecules reveal the emission brightening analogous to the effect observed for [001] molecules (Fig. 17). There are however notable differences. The first is that the effect is much stronger than in the case of the [001] growth. Namely, the dark exciton oscillator strength reaches even up to 1/2500 fraction of the bright exciton of the same system. This surprisingly large value could allow for the direct observation of the dark exciton in the typical photoluminescence experiment, even without the application of external fields. Secondly, the dark exciton emission is in-plane polarized, i.e., it has the same polarization as the bright exciton. Such polarization properties (and energy splittings) are in principle predicted [63] by the group theory for all C_{3v} nanostructures with a heavy-hole exciton and confirmed by our atomistic approach. Both of these features are of large practical importance for potential dark exciton applications in the field of quantum optics [11–13]. Finally, we emphasize that quantum dot molecule studies in this paper offer a unique possibility of tailoring dark exciton spectra by tuning the interdot distance.

Nonidentical quantum dots

Next, in Fig. 18 we present the single particle energy spectra of a [111] quantum dot molecule formed by quantum dots of different height ($h = 2.8$ and $h = 2.1$ nm; 8 and

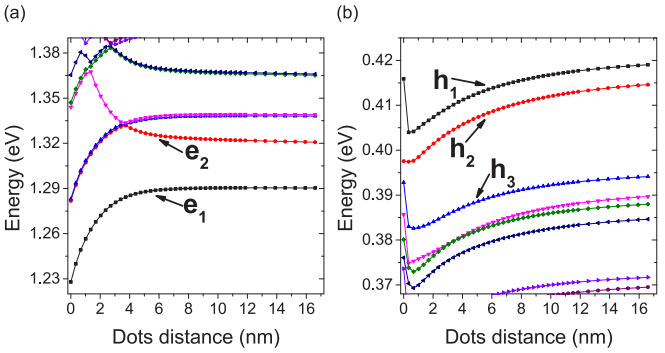

FIG. 18. Single particle electron (a) and hole (b) spectra calculated for a nanowire quantum dot molecule formed by two disk shaped InAs quantum dots of different height (see the text) on a [111] oriented InP substrate.

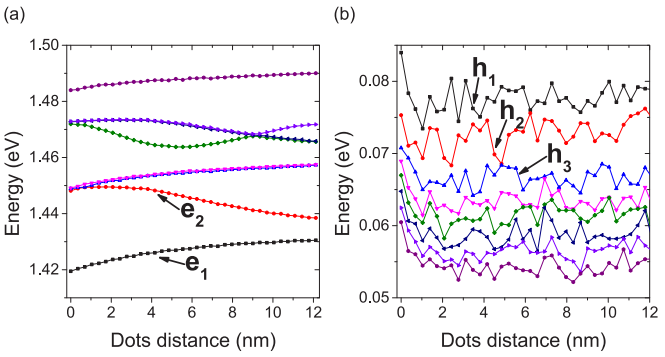

FIG. 19. Single particle electron (a) and hole (b) spectra calculated for an alloyed nanowire quantum dots molecule formed by two disk shaped $InAs_{0.2}P_{0.8}$ quantum dots of different height (see the text) on a [111] oriented InP substrate.

6 monolayers along [111] correspondingly; Fig. 11). These spectra resemble that of identical [111] double quantum dots, yet with significantly reduced interdot coupling and limited formation of molecular like orbitals (Figs. 13 and 14).

A notable difference between [001] and [111] quantum dot molecules is that the [111] grown nanostructure formed by two nonidentical dots, such as quantum dots of different height, will remain the same overall atomistic symmetry C_{3v} as the [111] system formed by identical quantum dots. Therefore the excitonic spectra of a [111] heterodot is qualitatively identical to that of a [111] homodot system [Fig. 17(b)]. The increase of the optical activity of the dark exciton appears somewhat (by factor three) reduced compared to a system formed by identical quantum dots, yet still far more pronounced than in [001] quantum dot molecules. Our results indicate thus that the increase of dark exciton activity in [111] quantum dot molecules should be resistant with respect to fluctuations of individual quantum dot heights, which may naturally occur during the growth process. Such fluctuations will also not affect the vanishing fine structure splitting of both bright and dark excitons in quantum dot molecules, since (neglecting alloying) this property is protected by the C_{3v} symmetry irrespectively from individual quantum dot heights (or diameters).

IV. ALLOYED QUANTUM DOT MOLECULES

Experimentally grown nanostructures are never free from the effects of alloying [67] and thus related alloy randomness. These are effectively lowering nanostructure symmetry and differentiating its properties from the idealistic group theory picture. In particular, due to specifics of the VLS growth, the chemical composition of realistic nanowire quantum dots varies strongly from pure InAs with a profound content of the barrier material (InP) reaching up to 80% [76]. Whereas there is significant progress [7] in the controlled growth of high quality nanowire quantum dots, the alloying currently seems unavoidable. Therefore in this work we additionally study spectral properties of the same quantum dot molecules as studied above, however with different chemical composition, i.e., instead of pure InAs we consider now quantum dots molecules formed by $InAs_{0.2}P_{0.8}$ embedded in an InP nanowire. For comparison we have also run calculations for a case with 50% contribution of phosphorous, namely $InAs_{0.5}P_{0.5}$ quantum dots. In all cases we assumed uniform composition profiles with phosphorous atoms distributed evenly over quantum dot volumes. We note that our results were obtained by generating one random sample corresponding to one interdot distance. One could go further and generate many different random samples for each nanostructure in a similar way to that of Ref. [42]. Such study goes however beyond the scope of the current paper and will be published elsewhere in the near future.

Quasimolecules of mixed composition and composed of different height quantum dots present the most realistic case, since in the experiment one should always expect intermixing and fluctuations of quantum dot dimensions. Thus here we present results for the case of a [111] quantum dot molecule formed by nonidentical quantum dots ($h = 2.8$ and $h = 2.1$ nm; 8 and 6 monolayers along [111] correspondingly; $d = 18$ nm). However, we have additionally performed calculations (not shown here) for all systems considered earlier (i.e., identical quantum dots and [001] nanowire orientation), and we have found that effects of alloy randomness and composition intermixing are qualitatively similar in all considered cases. Results of calculations for a [111] of alloyed nonidentical quantum dot forming a molecule are shown in Fig. 19 for the single particle spectra and in Figs. 20 and 21 for the many-body excitonic spectra.

The effect of alloying on the electron spectra leads first of all to the blueshift of the electron energies due to an add-mixture of large band gap (InP) material in the dot region. Additionally, the presence of the barrier material in the quantum dot effectively reduces the confinement and leads to reduced level spacings as seen in Fig. 19. The shallow confinement of the intermix system leads additionally to large spatial delocalization and thus increased electron states interdot coupling, which is of long range character and is present even for the highest considered interdot distances. Interestingly alloy randomness appears to have a limited effect on the electron energies evolution, partially due to larger electron levels spacings as compared to hole levels spacings. On the other hand variations of single particle hole energies due to alloy randomness seem to dominate their spectra, with

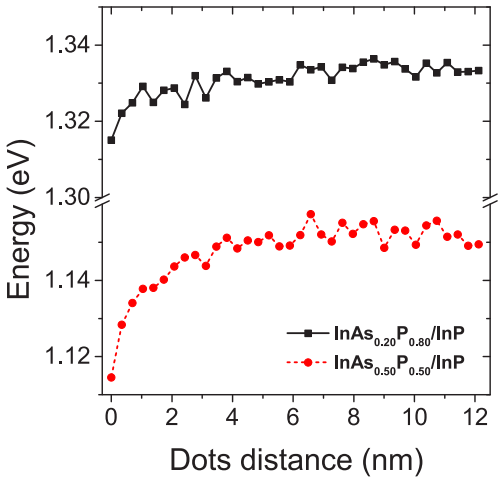

FIG. 20. The ground exciton state energy calculated for alloyed nanowire quantum dots molecule formed by two disk shaped quantum dots of different height (see the text) on [111] oriented InP substrate. Black/squares/straight line represent $InAs_{0.2}P_{0.8}$ case, whereas red/cirecles/dashed line corresponds to $InAs_{0.5}P_{0.5}$ systems.

no clear distance-dependent trend visible in the large range of interdot spacings. These profound variations of single particle (especially hole) energies (as well as of electron-hole Coulomb matrix elements—not shown here) have a strong effect on the excitonic spectra, as they lead to significant variations of the excitonic energies (Fig. 20) on top of the distance dependence. This is a hallmark of lattice (alloy) randomness which is always present in realistic excitonic spectra. Similar effects has been observed in numerous other nanostructures varying from typical self-assembled quantum dots [44,45] to such peculiar systems as natural quantum dots [42] or quantum dashes [43]. Finally, the blueshift of single particle energies leads to a corresponding blueshift of excitonic energies, which is proportional to phosphorous content, reaching 1.15 eV for $InAs_{0.5}P_{0.5}$ quantum dot molecule and going above 1.4 eV for the $InAs_{0.2}P_{0.8}$ case (Fig. 20). The distance dependence of excitonic energies is rather weak, due to shallow confinement and delocalization of single particle electron states. This is

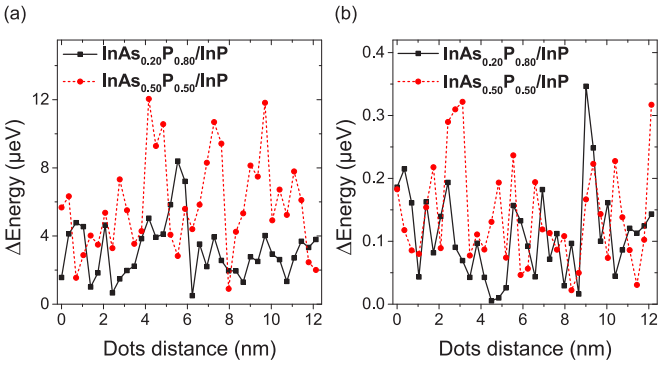

FIG. 21. The bright (a) and dark (b) exciton splitting for an alloyed nanowire quantum dots molecule formed by two disk shaped quantum dots of different height (see the text) on a [111] oriented InP substrate. Black/squares/straight line represent the $InAs_{0.2}P_{0.8}$ case, whereas red/circles/dashed line corresponds to $InAs_{0.5}P_{0.5}$ systems.

especially visible in the highly alloyed case ($InAs_{0.2}P_{0.8}$) where there is less than 10 meV redshift of excitonic energy when comparing large and short quantum dots distances, compared to about 30 meV redshift in the $InAs_{0.5}P_{0.5}$ case. At the same time both values are far smaller than that of well confined electron states in pure InAs quantum dot molecules discussed earlier, where the energy shift due to interdot coupling was reaching up to 80 meV.

Apart from the main spectral features, the alloy randomness affects the excitonic fine structure as well. Alloying breaks the perfect C_{3v} symmetry (which is now reduced to C_1) and therefore it breaks both the bright and the dark exciton degeneracy leading to the splitting of both excitonic species. The magnitude of the bright exciton splitting (Fig. 21) varies from 0.5 μeV up to even 12 μeV, which is comparable to experimental results for single nanowire quantum dots (compare Fig. 4(e) of supporting information of Ref. [6]). Additionally the bright exciton splitting is dominated by randomness and does not show a clear trend with the interdot distance. Generally the bright exciton splitting is larger for the case $InAs_{0.5}P_{0.5}$ corresponding to the maximally disordered case, which shows a key role of composition dependent intermixing on the fine structure spectra. In the $InAs_{0.5}P_{0.5}$ case the average bright exciton splitting calculated over all interdot distances is 5.8 μeV (with a standard deviation of 2.8 μeV), whereas in the $InAs_{0.2}P_{0.8}$ quantum dot molecule it is 3.2 μeV (and 1.7 μeV standard deviation). The dark exciton splitting (Fig. 21) shows similar behavior, with no apparent distance dependence, and a magnitude of splitting never exceeding 0.35 μeV. Our results clearly indicate that lattice randomness due to alloying presents a possible challenge in achieving vanishing fine structure and hence entangled photon generation in nanowire quantum dot molecules. Similar limitations were found by the empirical pseudopotential method for self-assembled quantum dots [77], whereas for nanowire quantum dots the same method predicts vanishing bright exciton splitting even for intermixed nanowire quantum dots [3]. However the empirical pseudopotential method systematically underestimates the bright exciton splitting compared to experiment [78] and other atomistic calculations such as the tight-binding method [4,40]. In reality in order to achieve a working nanodevice based on nanowire quantum dots one needs to select a nanostructure out of many samples, some of which have large bright excitons splitting even exceeding 10 μeV (supporting information of Ref. [6]). The same effect of alloying should be thus expected for nanowire quantum dot molecules as confirmed by our atomistic calculations.

Finally, Figs. 22 and 23 show both optical and energy spectra of the dark and bright excitons in alloyed quantum dot molecules of $InAs_{0.2}P_{0.8}$ and $InAs_{0.5}P_{0.5}$ compositions correspondingly. The light emitted from the bright (and dark) excitons is linearly and mostly in-plane polarized, there is however a significant out-of-plane (z) component due to symmetry reduction by the intermixing. Moreover the polarization directions in the quantum dot plane are practically randomized and vary from system to system. Oscillator strengths in Figs. 22 and 23 were calculated for polarizations corresponding to maximum intensity of a given system, yet we reiterate that polarization angles (axis) are randomized. Similar to previous cases there is a dip in the "bright"/"dark" exchange splitting

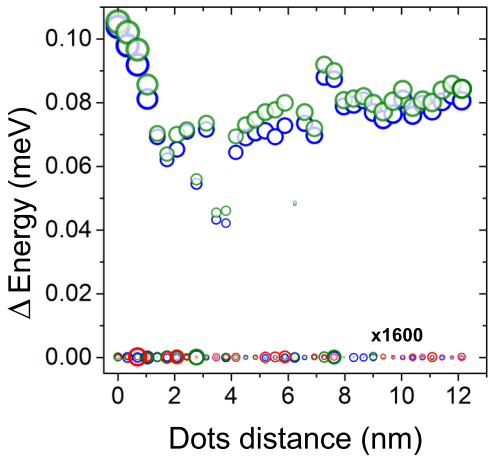

FIG. 22. The bright and dark exciton energy and optical spectra calculated for alloyed nanowire quantum dots molecule formed by two disk shaped $InAs_{0.2}P_{0.8}$ quantum dots of different height (see the text) on a [111] oriented InP substrate. The blue and green circle correspond to different (random) in-plane orthogonal polarizations, whereas red circles correspond to the out-of-plane (z) polarization. The size (area) of the circles is proportional to the oscillator strength. Energies are measured with respect to the ground excitonic ("dark") state.

due to the interdot coupling, however the general behavior with distance is smeared by the effects of alloy randomness, with exchange splitting varying between 40 and 100 μeV in the $InAs_{0.2}P_{0.8}$ case. The distance dependence is more pronounced for a less alloyed $InAs_{0.5}P_{0.5}$ quantum dot molecule (Fig. 23), where the exchange splitting is actually bigger and it drops

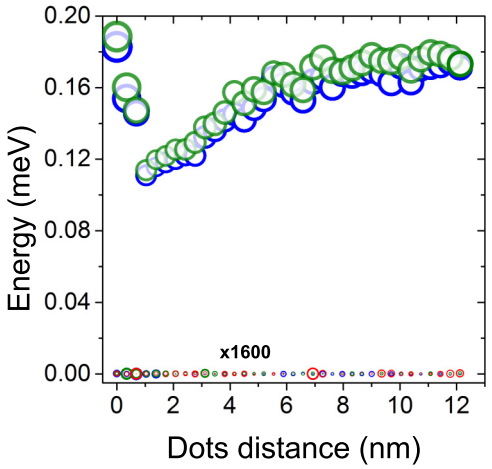

FIG. 23. The bright and dark exciton energy and optical spectra calculated for an alloyed nanowire quantum dots molecule formed by two disk shaped $InAs_{0.5}P_{0.5}$ quantum dots of different height (see the text) on a [111] oriented InP substrate. Th blue and green circle correspond to different (random) in-plane orthogonal polarizations, whereas red circles correspond to the out-of-plane (z) polarization. The size (area) of the circles is proportional to the oscillator strength. Energies are measured with respect to the ground excitonic ("dark") state.

from 180 μeV for the largest interdot separation to 110 μeV at 1 nm quantum dots distance.

Importantly, the effect of dark exciton brightening is still present in highly alloyed quantum dot molecules, however is also reveals only a weak trend on the interdot separation. The dark exciton emission appears to be somewhat more pronounced for distances between 1 and 3 nm nanometers (Fig. 22), however there is also a significant dark exciton optical activity at other distances, e.g., at $\approx$7.5 nm. Additionally there is a non-negligible dark exciton activity for the case of merged (single) quantum dot ($d = 0$) or highly separated quantum dots ($d > 10$ nm). Typically in alloyed cases the dark exciton oscillator strengths, for both in-plane and out-of-plane polarizations, vary between 10^{-4} to about 0.4×10^{-3} fraction of the bright exciton oscillator strength. The magnitude of the brightening is therefore comparable to nonalloyed cases, however the dark exciton polarization directions are now effectively randomized by the lattice intermixing. Alloyed quantum dots can thus be considered as systems of highly-mixed angular momenta, and thus strict selection rules obtained for pure InAs quantum dots are no longer exactly true. Therefore transitions nominally forbidden in the idealized, high-symmetry cases can now be optically allowed and actually even enhanced by lattice randomness due to alloying. Our calculations thus indicate that apart from control of interdot distance in nanowire quantum dot molecules, the control of quantum dot molecule composition allows for tailoring optical and energy spectra of these molecules and in particular the excitonic fine structure and oscillator strengths.

V. SUMMARY

We have presented results of atomistic tight-binding calculations for InAs/InP nanowire quantum dot molecules. We have studied numerous cases differing by interdot distance and substrate orientation of a host nanowire. We have also calculated properties of quantum dot molecules with intermixed (alloyed) composition. Further, we have focused our attention on the details of the excitonic spectra, in particular the excitonic fine structure. Our computations indicate that despite the cylindrical shape symmetry, in a case of [001] substrate orientation, the exciton confined in the double quantum dot system reveals the bright exciton splitting, provided that quantum dots forming a molecule are of different height. The individual quantum dots may share the same diameter and cylindrical shape, yet the difference in heights triggers the vertical inversion asymmetry, reduces the overall symmetry to C_{2v}, and finally leads to a nonvanishing fine structure splitting. Nanowire quantum dot molecules formed by identical [001] quantum dots reveal no fine structure splitting as they are protected by their high D_{2d} symmetry. On the other hand, we have found that quantum dot molecules grown on a [111] substrate have C_{3v} symmetry even in the case of different heights of individual dots. Their bright and dark exciton spectra remain degenerate, and these degeneracies are protected by high overall symmetry for all considered interdot spacings. Interestingly, C_{3v} systems, whether the dots are identical or different, do not have vertical inversion symmetry and that leads to the reduction of interdot coupling and increased localization of single particle states inside of individual dots

rather than formation of delocalized orbitals. Next, we have found a significant (by many orders of magnitude) increase of the dark exciton optical activity in double quantum dots as compared to a single nanowire quantum dot. For a [001] double quantum dot system the dark exciton oscillator strengths can reach a significant 10^{-4} fraction of the bright exciton due. For [111] cases the optical activity of the dark exciton is even stronger reaching even up to 1/2500 fraction of the bright exciton. Such strong dark exciton activity can find potential application in quantum information, as it can be tailored by tuning interdot distance. Finally, we have calculated properties of quantum dot of realistic intermixed composition, and we have shown the lattice randomness due to alloying triggers the fine structure splitting of both bright and dark exciton, enhances dark exciton optical activity, as well as randomizes polarization directions of excitonic states, which additionally gain a non-negligible out-of-plane contribution.

Note added in proof. Recently, we became aware of Ref. [79]. There, InAsP nanowire quantum dot molecules were obtained experimentally. Such quantum dots are similar to those studied theoretically in our paper confirming further the possibility of achieving InAs double quantum dot systems in InP nanowires.

ACKNOWLEDGMENT

M.Z. acknowledges support from the Polish National Science Centre based on decision No. 2015/18/E/ST3/00583.

[1] L. Jacak, P. Hawrylak, and A. Wojs, *Quantum Dots* (Springer, Berlin, 1998).
[2] M. T. Borgström, V. Zwiller, E. Müller, and A. Imamoglu, Nano Lett. **5**, 1439 (2005).
[3] R. Singh and G. Bester, Phys. Rev. Lett. **103**, 063601 (2009).
[4] M. Zieliński, Phys. Rev. B **88**, 155319 (2013).
[5] O. Benson, C. Santori, M. Pelton, and Y. Yamamoto, Phys. Rev. Lett. **84**, 2513 (2000).
[6] M. A. M. Versteegh, M. E. Reimer, K. D. Jöns, D. Dalacu, P. J. Poole, A. Gulinatti, A. Giudice, and V. Zwiller, Nat. Commun. **5**, 5298 (2014).
[7] D. Dalacu, K. Mnaymneh, J. Lapointe, X. Wu, P. J. Poole, G. Bulgarini, V. Zwiller, and M. E. Reimer, Nano Lett. **12**, 5919 (2012).
[8] M. E. Reimer, G. Bulgarini, N. Akopian, M. Hocevar, M. B. Bavinck, M. A. Verheijen, E. P. A. M. Bakkers, L. P. Kouwenhoven, and V. Zwiller, Nat. Commun. **3**, 737 (2012).
[9] These are in fact double groups, but following references [3,64], and for simplicity we use single groups notation.
[10] M. Bayer, G. Ortner, O. Stern, A. Kuther, A. A. Gorbunov, A. Forchel, P. Hawrylak, S. Fafard, K. Hinzer, T. L. Reinecke, S. N. Walck, J. P. Reithmaier, F. Klopf, and F. Schäfer, Phys. Rev. B **65**, 195315 (2002).
[11] I. Schwartz, E. R. Schmidgall, L. Gantz, D. Cogan, E. Bordo, Y. Don, M. Zielinski, and D. Gershoni, Phys. Rev. X **5**, 011009 (2015).
[12] I. Schwartz, D. Cogan, E. R. Schmidgall, L. Gantz, Y. Don, M. Zieliński, and D. Gershoni, Phys. Rev. B **92**, 201201 (2015).
[13] M. Zieliński, Y. Don, and D. Gershoni, Phys. Rev. B **91**, 085403 (2015).
[14] H. J. Krenner, M. Sabathil, E. C. Clark, A. Kress, D. Schuh, M. Bichler, G. Abstreiter, and J. J. Finley, Phys. Rev. Lett. **94**, 057402 (2005).
[15] N. N. Ledentsov, V. A. Shchukin, M. Grundmann, N. Kirstaedter, J. Böhrer, O. Schmidt, D. Bimberg, V. M. Ustinov, A. Y. Egorov, A. E. Zhukov, P. S. Kop'ev, S. V. Zaitsev, N. Y. Gordeev, Z. I. Alferov, A. I. Borovkov, A. O. Kosogov, S. S. Ruvimov, P. Werner, U. Gösele, and J. Heydenreich, Phys. Rev. B **54**, 8743 (1996).
[16] H. J. Krenner, E. C. Clark, T. Nakaoka, M. Bichler, C. Scheurer, G. Abstreiter, and J. J. Finley, Phys. Rev. Lett. **97**, 076403 (2006).
[17] E. A. Stinaff, M. Scheibner, A. S. Bracker, I. V. Ponomarev, V. L. Korenev, M. E. Ware, M. F. Doty, T. L. Reinecke, and D. Gammon, Science **311**, 636 (2006).
[18] M. F. Doty, J. I. Climente, A. Greilich, M. Yakes, A. S. Bracker, and D. Gammon, Phys. Rev. B **81**, 035308 (2010).
[19] P. L. Ardelt, K. Gawarecki, K. Müller, A. M. Waeber, A. Bechtold, K. Oberhofer, J. M. Daniels, F. Klotz, M. Bichler, T. Kuhn, H. J. Krenner, P. Machnikowski, and J. J. Finley, Phys. Rev. Lett. **116**, 077401 (2016).
[20] M. F. Doty, J. I. Climente, M. Korkusinski, M. Scheibner, A. S. Bracker, P. Hawrylak, and D. Gammon, Phys. Rev. Lett. **102**, 047401 (2009).
[21] M. F. Doty, M. Scheibner, I. V. Ponomarev, E. A. Stinaff, A. S. Bracker, V. L. Korenev, T. L. Reinecke, and D. Gammon, Phys. Rev. Lett. **97**, 197202 (2006).
[22] G. Ortner, M. Bayer, Y. Lyanda-Geller, T. L. Reinecke, A. Kress, J. P. Reithmaier, and A. Forchel, Phys. Rev. Lett. **94**, 157401 (2005).
[23] B. W. Lovett, J. H. Reina, A. Nazir, and G. A. D. Briggs, Phys. Rev. B **68**, 205319 (2003).
[24] J. Planelles, F. Rajadell, and J. I. Climente, Phys. Rev. B **92**, 041302 (2015).
[25] W. Jaskólski, M. Zieliński, G. W. Bryant, and J. Aizpurua, Phys. Rev. B **74**, 195339 (2006).
[26] W. Jaskólski, M. Zieliński, and G. W. Bryant, Acta Phys. Pol. A **106**, 193 (2004).
[27] G. Bester, A. Zunger, and J. Shumway, Phys. Rev. B **71**, 075325 (2005).
[28] D. Bimberg, M. Grundmann, and N. Ledentsov, *Quantum Dot Heterostructures* (Wiley, Chichester, 1999).
[29] G. Priante, F. Glas, G. Patriarche, K. Pantzas, F. Oehler, and J.-C. Harmand, Nano Lett. **16**, 1917 (2016).
[30] G. Priante, G. Patriarche, F. Oehler, F. Glas, and J.-C. Harmand, Nano Lett. **15**, 6036 (2015).
[31] R. S. Wagner and W. C. Ellis, Appl. Phys. Lett. **4**, 89 (1964).
[32] L. E. Jensen, M. T. Bjrk, S. Jeppesen, A. I. Persson, B. J. Ohlsson, and L. Samuelson, Nano Lett. **4**, 1961 (2004).
[33] K. Leung and K. B. Whaley, Phys. Rev. B **56**, 7455 (1997).
[34] S. Lee, L. Jönsson, J. W. Wilkins, G. W. Bryant, and G. Klimeck, Phys. Rev. B **63**, 195318 (2001).
[35] R. Santoprete, B. Koiller, R. B. Capaz, P. Kratzer, Q. K. K. Liu, and M. Scheffler, Phys. Rev. B **68**, 235311 (2003).

[36] M. Usman, Phys. Rev. B **86**, 155444 (2012).
[37] S. Schulz, S. Schumacher, and G. Czycholl, Phys. Rev. B **73**, 245327 (2006).
[38] M. Zieliński, M. Korkusinski, and P. Hawrylak, Phys. Rev. B **81**, 085301 (2010).
[39] M. Zieliński, Phys. Rev. B **86**, 115424 (2012).
[40] M. Zieliński, J. Phys.: Condens. Matter **25**, 465301 (2013).
[41] P. T. Różański and M. Zieliński, Phys. Rev. B **94**, 045440 (2016).
[42] M. Zieliński, K. Gołasa, M. R. Molas, M. Goryca, T. Kazimierczuk, T. Smoleński, A. Golnik, P. Kossacki, A. A. L. Nicolet, M. Potemski, Z. R. Wasilewski, and A. Babiński, Phys. Rev. B **91**, 085303 (2015).
[43] P. Mrowinski, M. Zieliński, M. Świderski, J. Misiewicz, A. Somers, J. P. Reithmaier, S. Höfling, and G. Sek, Phys. Rev. B **94**, 115434 (2016).
[44] V. Mlinar, M. Bozkurt, J. M. Ulloa, M. Ediger, G. Bester, A. Badolato, P. M. Koenraad, R. J. Warburton, and A. Zunger, Phys. Rev. B **80**, 165425 (2009).
[45] V. Mlinar and A. Zunger, Phys. Rev. B **80**, 205311 (2009).
[46] P. N. Keating, Phys. Rev. **145**, 637 (1966).
[47] R. M. Martin, Phys. Rev. B **1**, 4005 (1970).
[48] C. Pryor, J. Kim, L. W. Wang, A. J. Williamson, and A. Zunger, J. Appl. Phys. **83**, 2548 (1998).
[49] T. Saito and Y. Arakawa, Physica E **15**, 169 (2002).
[50] D. J. Chadi, Phys. Rev. B **16**, 790 (1977).
[51] J.-M. Jancu, R. Scholz, F. Beltram, and F. Bassani, Phys. Rev. B **57**, 6493 (1998).
[52] S. Lee, F. Oyafuso, P. von Allmen, and G. Klimeck, Phys. Rev. B **69**, 045316 (2004).
[53] M. Zieliński, Acta Phys. Pol. A **122**, 312 (2012).
[54] M. Gong, K. Duan, C.-F. Li, R. Magri, G. A. Narvaez, and L. He, Phys. Rev. B **77**, 045326 (2008).
[55] A. Schliwa, M. Winkelnkemper, and D. Bimberg, Phys. Rev. B **76**, 205324 (2007).
[56] Edited by P. Michler, *Topics in Applied Physics*, Vol. 90 (Springer, New York, 2003).
[57] W. Sheng, S.-J. Cheng, and P. Hawrylak, Phys. Rev. B **71**, 035316 (2005).
[58] A. Franceschetti, L. W. Wang, H. Fu, and A. Zunger, Phys. Rev. B **58**, R13367 (1998).
[59] S. V. Goupalov and E. L. Ivchenko, Phys. Solid State **43**, 1867 (2001).
[60] C. Delerue and M. Lannoo, *Nanostrucutres: Theory and Modelling*, Nanosciences and Technology Series (Springer, New York, 2004).
[61] M. Bayer, P. Hawrylak, K. Hinzer, S. Fafard, M. Korkusinski, Z. R. Wasilewski, O. Stern, and A. Forchel, Science **291**, 451 (2001).
[62] J. I. Climente, M. Korkusinski, G. Goldoni, and P. Hawrylak, Phys. Rev. B **78**, 115323 (2008).
[63] K. F. Karlsson, M. A. Dupertuis, D. Y. Oberli, E. Pelucchi, A. Rudra, P. O. Holtz, and E. Kapon, Phys. Rev. B **81**, 161307 (2010).
[64] M. A. Dupertuis, K. F. Karlsson, D. Y. Oberli, E. Pelucchi, A. Rudra, P. O. Holtz, and E. Kapon, Phys. Rev. Lett. **107**, 127403 (2011).
[65] M. Korkusinski and P. Hawrylak, Phys. Rev. B **87**, 115310 (2013).
[66] M. Korkusinski, M. Zieliński, and P. Hawrylak, J. Appl. Phys. **105**, 122406 (2009).
[67] D. Dalacu, A. Kam, D. G. Austing, X. Wu, J. Lapointe, G. C. Aers, and P. J. Poole, Nanotechnology **20**, 395602 (2009).
[68] A. Schliwa, M. Winkelnkemper, A. Lochmann, E. Stock, and D. Bimberg, Phys. Rev. B **80**, 161307 (2009).
[69] S. Schulz, M. A. Caro, E. P. O'Reilly, and O. Marquardt, Phys. Rev. B **84**, 125312 (2011).
[70] S. Tomi and N. Vukmirovi, J. Appl. Phys. **110**, 053710 (2011).
[71] O. Marquardt, S. Schulz, C. Freysoldt, S. Boeck, T. Hickel, E. P. O'Reilly, and J. Neugebauer, Opt. Quantum Electron. **44**, 183 (2011).
[72] A. De and C. E. Pryor, Phys. Rev. B **81**, 155210 (2010).
[73] L. Zhang, J.-W. Luo, A. Zunger, N. Akopian, V. Zwiller, and J.-C. Harmand, Nano Lett. **10**, 4055 (2010).
[74] W. Sheng and J.-P. Leburton, Appl. Phys. Lett. **81**, 4449 (2002).
[75] Please note reverse energy ordering of hole states, i.e., single particle hole state energies effectively enter the excitonic Hamiltonian with a negative sign.
[76] M. Bouwes Bavinck, M. Zieliski, B. J. Witek, T. Zehender, E. P. A. M. Bakkers, and V. Zwiller, Nano Lett. **12**, 6206 (2012).
[77] R. Singh and G. Bester, Phys. Rev. Lett. **104**, 196803 (2010).
[78] R. Singh and G. Bester, Phys. Rev. B **84**, 241402 (2011).
[79] M. Khoshnegar, T. Huber, A. Predojević, D. Dalacu, M. Prilmüller, J. Lapointe, X. Wu, P. Tamarat, B. Lounis, P. Poole, G. Weihs, and H. Majedi, arXiv:1510.05898v2 [quant-ph].